A&A manuscript no.
(will be inserted by hand later)

Your thesaurus codes are:
04(3.13.2, 08.08.1, 10.19.2, 10.19.3)

ASTRONOMY
AND
ASTROPHYSICS
1.2.2008

On the extinction towards Baade's Window

Y.K. Ng[1] **and G. Bertelli**[2,3]

[1] IAP, CNRS, 98 bis Boulevard Arago, 75014 Paris, France (E-mail: ng@iap.fr)
[2] Department of Astronomy, Vicolo dell'Osservatorio 5, 35122 Padua, Italy (bertelli@astrpd.pd.astro.it)
[3] National Council of Research, CNR – GNA, Rome, Italy

Received 16 April 1996 / Accepted 5 May 1996

Abstract. An analysis is made on the morphology of the sequences, formed by stars distributed along the line of sight in (V,V–I) CMDs (Colour Magnitude Diagram) from Baade's Window (l=1.°0, b=−3.°9). The extinction is due to an absorbing layer with an effective thickness of about 100 pc. A linearly, with distance, increasing extinction up to a maximum value inside the absorbing layer is in first order a good approximation for the actual extinction present along the line of sight.

We show that the morphology of the disc sequence gives a good indication of the nearby extinction along the line of sight. The morphology of the bulge/bar red horizontal branch is likely due to a combination of differential reddening and a significant metallicity spread among the horizontal branch stars. This is irrespective of the type of extinction law adopted. There is in Baade's Window globally no big difference between a Poissonian or a patchy type of extinction, except for substructures in the morphology of the sequences for the latter.

Key words: methods: data analysis – Stars: HR-Diagram – Galaxy: stellar content, structure

1. Introduction

Synthetic Hertzsprung-Russell Diagrams (HRDs) can be generated through the population synthesis technique, with the aid of libraries of stellar evolution tracks (Bertelli et al. 1994a) of different chemical compositions These HR-diagrams are part of a powerful tool, the HRD-GST (HRD Galactic Software Telescope; see Ng 1994 & 1996 and Ng et al. 1995 for details), in stars counts studies of the Galactic Structure, in particular the structure towards the Galactic Centre. Using the HRD-GST, the contributions of various stellar populations are decomposed statistically. Through a detailed and a concise analysis of the star counts along the line of sight we aim to study

- the galactic structure;
- the interstellar extinction; and
- the ages and metallicities of the different stellar populations.

The results from our studies are reported in the papers by Ng et al. (1995 & 1996a), Bertelli et al. (1995), these papers will be hereafter referred to as Paper I–III, and Bertelli et al. (1996) & Ng et al. (1996b).

The ages, metallicities and the spatial distributions of the stars from various populations contain a wealth of information about the formation and evolution of our Galaxy. The stars, observed along any line of sight, are the result of a complex mixture from various populations. Especially towards the Galactic Centre there appears to be no clear consensus about the ages & metallicities of the stellar populations (disc, bulge, bar ...) and the parameterization of the galactic structure. The large variation of the extinction over a relative small area is one of the major causes. The near-IR passbands are less sensitive to extinction. Each field needs to be studied separately, because the extinction over the various fields is not easily parameterized. The best strategy is probably, to determine the extinction (if this is not too high and/or patchy) & the age-metallicity of the various stellar populations from the optical passbands and verify the results with near-IR photometry.

In (V,V–I) CMDs extinction and age-metallicity effects are difficult to separate from each other. The tilted clump of HB (Horizontal Branch) stars could be due to large differential extinction, a large metallicity spread of the HB stars, or a combination of both (Catalan & de Freitas Pacheco 1996; Ortolani et al. 1990 & 1995a; Ng et al. 1996a&d). This might imply, as suggested by Renzini (1995), that there are no super metal-rich stars towards the Galactic Centre. Patchy extinction might explain the various structures present in the (V,V–I) CMDs. In addition the metal-rich globular clusters might be related to the bulge (Ortolani et al. 1995a) or the bar (Ng et al. 1996d) in both age & metallicity. Establishment to which population these clusters are related with, would provide valuable information about part of the formation history of our present day Galaxy.

The objective of this paper is to show, how the HRD-GST deals with extinction and to analyze the influence of the various manifestations of the extinction. Emphasis is put on the extinction in the optical passbands and on the morphological

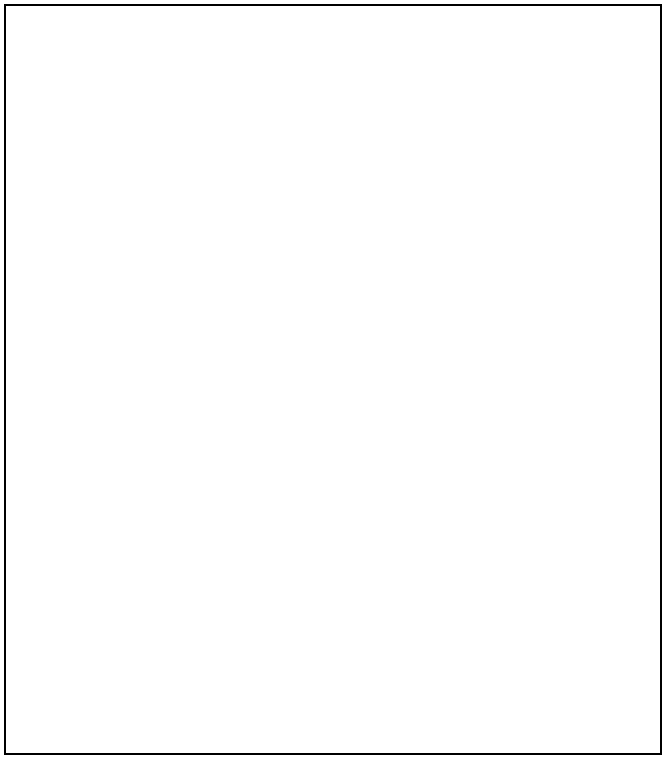

Fig. 1.1. (Synthetic (V,V–I) CMD for Baade's Window. For sake of simplicity not all populations have been inserted. Only the disc populations with a scale height less than 250 pc and the 'bar' population (Ng et al. 1996a&c) are displayed. Dots, dashes, open circles and filled squares refer respectively to main sequence stars, core H-exhausted or red giant branch stars, horizontal branch stars and asymptotic giant branch stars

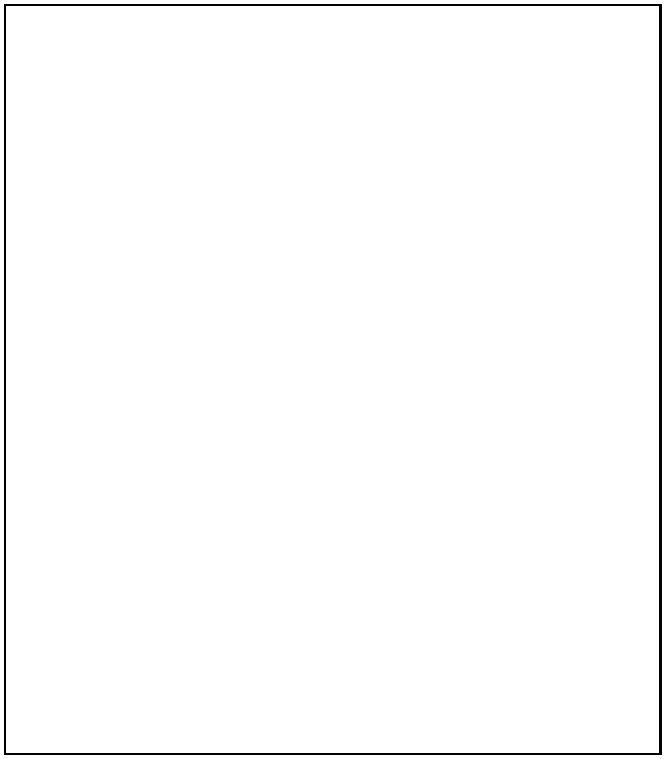

Fig. 1.2. Synthetic (V,V–I) CMD for Baade's Window in absence of extinction. For sake of simplicity not all populations have been inserted. Only the disc populations with a scale height less than 250 pc and the 'bar' population (Ng et al. 1996a&c) are displayed

appearance of the structures in the CMDs. We show what the effects are for a specific population. Baade's Window is used as an example. In contrast to Stanek (1996), we show which signatures can be expected in (V,V–I) CMDs from different types of extinction. Combination of the different morphological structures in the CMDs allows us to determine the extinction along the line of sight, see Bertelli et al. (1995) and Ng et al. (1996a&d). In Sect. 2 we describe our method, show the results and discuss them in Sect. 3. We end this paper with a summary of the results.

2. Extinction

2.1. Method

As starting and reference point we will use the extinction obtained from our analysis (Ng et al. 1996a) of Baade's Window CMD (Paczyński et al. 1994 and references cited therein). We use the extinction law $E_{V-I} = A_V/2.4$ to determine the extinction in the I passband. The analysis of Woźniak & Stanek (1996) justifies that this is a valid approach in Baade's Window. Figures 1.1 & 1.2 show the simulated CMDs for Baade's Window field, respectively with and without extinction along the line of sight. Figure 1.2 shows the change of the morphology in the CMD without extinction, indicating that the disc sequence provides useful indications about the nearby extinction along the line of sight. In this case almost all the structures move to bluer colours and brighter magnitudes. The disc sequence becomes a vertical structure, because we observe stars with the same colours at different distances. The dispersion is partly due to the photometric errors & the crowding simulation and partly due to age-metallicity differences among the disc stars. This figure also shows that, without extinction, the detection of the bar's main sequence turn-off could have been possible.

For sake of simplicity and clarity of the figures, in which the sensitivity is demonstrated to the foreground extinction, we considered only the foreground stars (i.e. populations with a scale height of 250 pc or less, say $d < 4$ kpc), together with the allegedly called 'bar' population. The contribution from other populations (old disc, thick disc, bulge, halo; see Ng et al. 1996b for a description of these population) have not been considered. The symbols in the figures designate approximately the evolutionary phase of each synthetic star. The extinction along the line of sight is varied in the following way:

- use a linear relation for the extinction curve between us and 1, 2 or 4 kpc; the extinction is taken equal to maximum value, $A_V = 1\overset{m}{.}75$, at the latter distances;
- use a step function for the extinction curve and increase the extinction to $A_V = 1\overset{m}{.}75$ at 1, 2 or 4 kpc away from us;

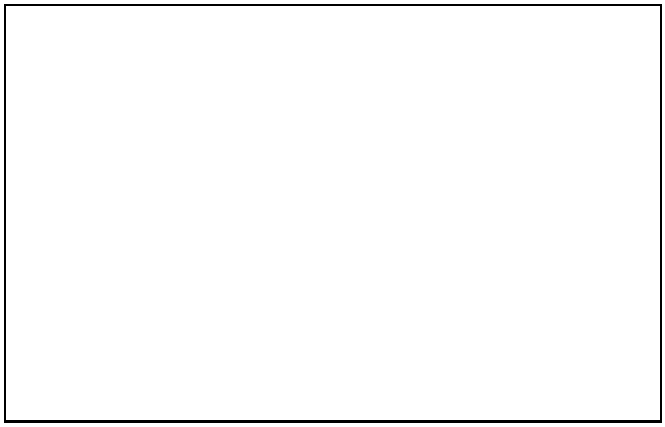

Fig. 2ab. The extinction along the line of sight in Baade's Window for various linearly (long-dashed line) and step-like (dashed line) increasing extinction curves, at respectively 1, 2 and 4 kpc away from us. The thick solid line is the mean extinction for subfield #3 (Ng et al. 1996a)

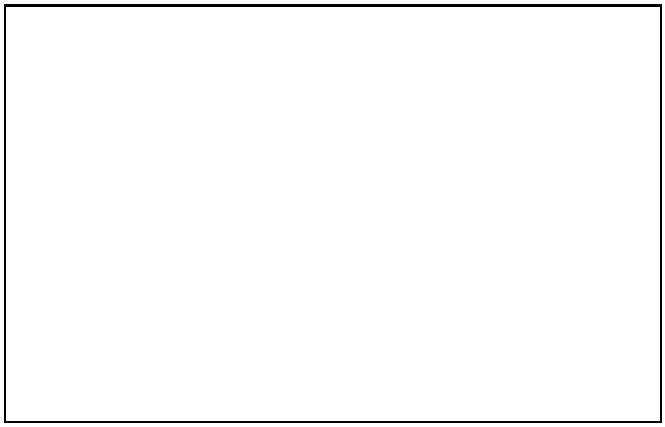

Fig. 2b. The extinction along the line of sight in Baade's Window for a Poissonian distribution ($A_V = 1\overset{m}{.}60 \pm 0\overset{m}{.}20$). The dots show the extinction from the synthetic stars 'detected' in the Monte-Carlo simulation. The thick solid line is the mean extinction for subfield #3 (Ng et al. 1996a)

- use a random extinction irrespective of the distance of the synthetic star along the line of sight; the distribution of the extinction is
  a) Poissonian, or
  b) patchy.

In the Poissonian case we assume the presence of an absorbing layer. For the effective thickness of this layer 100 pc (Cox 1989) is adopted. With an exponential density profile (Jones et al. 1981, Ruelas-Mayorga 1991) the extinction will be noticeable up to three times the effective thickness of this layer. We therefore use 300 pc as the boundary of this absorption layer. Outside this layer the extinction is equal to the maximum value. Inside this layer the extinction is scaled linearly with its distance. Arp (1965) showed that this is a valid approach for Baade's Window. This interpolation will suffice for the current purpose, see for example Figs. 2b & 2c.

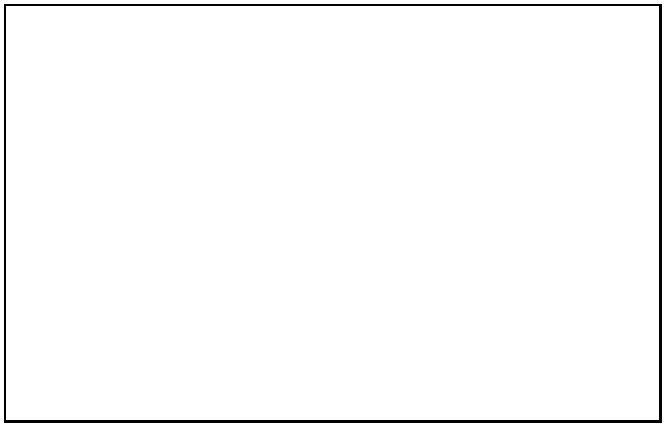

Fig. 2c. The extinction along the line of sight for a patchy ($\lambda = 0.6$; $A_V = 0\overset{m}{.}0 - 1\overset{m}{.}75$) distribution. Exaggerated, in order to enhance the contrast of the lumpiness. The dots show the extinction from the synthetic stars 'detected' in the Monte-Carlo simulation. It is emphasized that this does not represent the actual situation in Baade's Window. The thick solid line shows the mean extinction for Baade's Window subfield #3 (Ng et al. 1996a)

Several cases are considered for both the Poissonian and the patchy extinction. In the first case, the extinction is randomized between $A_V = 0\overset{m}{.}0 - 1\overset{m}{.}75$ and in the second case $A_V = 1\overset{m}{.}60 \pm 0\overset{m}{.}20$ is adopted. The first range, see Fig 2c, is not representative for the actual extinction in Baade's Window, because there are no regions where extinction is absent. It has been considered in order to exaggerate the difference between Poissonian and patchy extinction and furthermore, to enhance the contrast between the extinction clumps. The latter value covers approximately the range of mean extinction values determined for the Baade's Window subfields (Paczyński 1994, Ng et al. 1996a). For this part of the analysis the low and high extinction patches determined by Stanek (1996) are ignored. In first approximation, $A_V = 1\overset{m}{.}30 - 2\overset{m}{.}30$ is considered as a reasonable range for the total extinction range in Baade's Window.

A patchy extinction map is made with an algorithm, which generates N_1 clustered points around N_0 Poissonian distributed parent points. The N_1 points are uniformly distributed within a radius λ. This latter parameter defines the size of the extinction patch and is expressed in units of the mean distance between the centre positions of the patch centers. N_0 and N_1 define the resolution of the extinction map. Many different realizations can be made for different choices of the parameters. For our current purpose we made runs with relatively small & big patches by using $\lambda = 0.3$ and $\lambda = 0.6$.

Figures 2b & 2c show respectively, the Poissonian extinction and the patchy extinction. We emphasize that these figures show the total and not the differential extinction along the line of sight. Each dot represents the extinction assigned to a synthetic star in the simulations. Note that the extinction becomes clearer at larger distances, due to an increase in the detection of stars, which are located farther away in a larger volume.

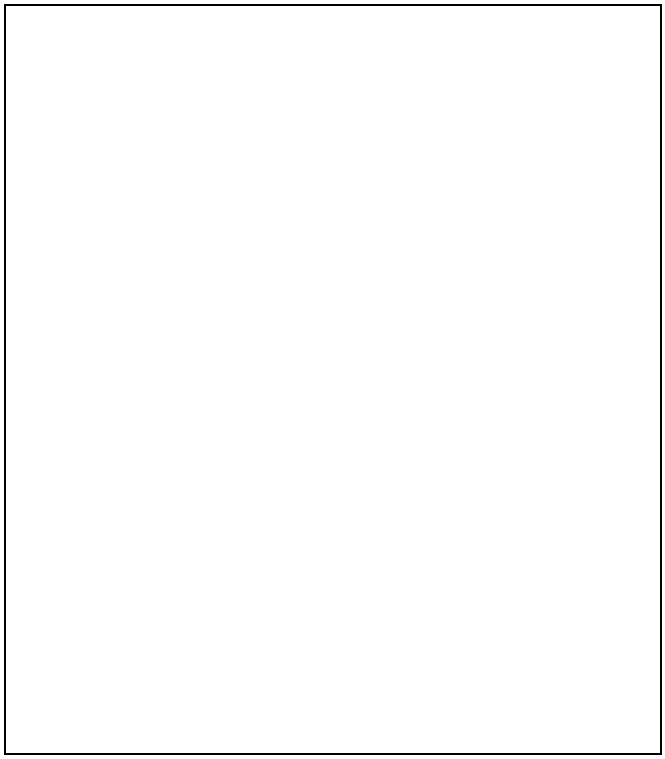

Fig. 3.1. Synthetic (V,V–I) CMD with a linearly increasing extinction up to $A_V = 1\overset{m}{.}75$ at 1 kpc distance

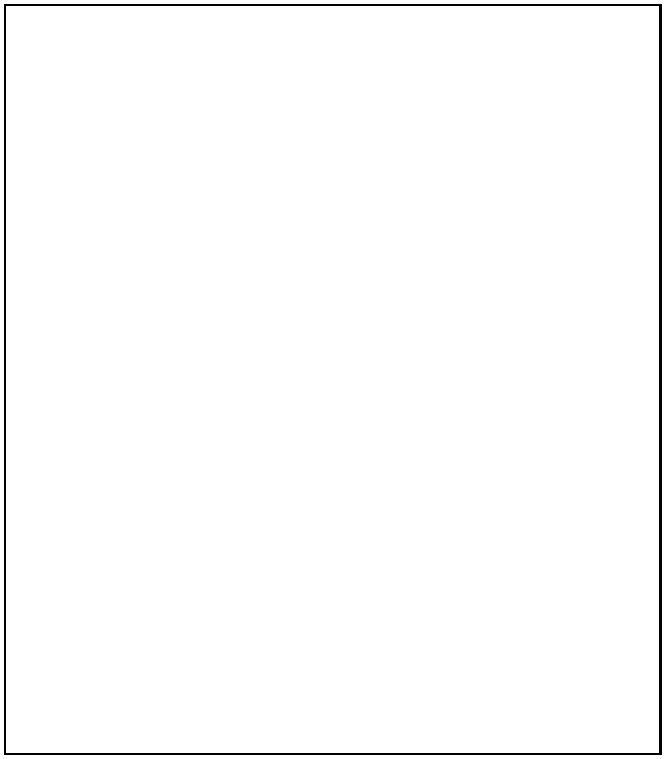

Fig. 3.2. Synthetic (V,V–I) CMD with a linearly increasing extinction up to $A_V = 1\overset{m}{.}75$ at 2 kpc distance

The large number of stars from the bar population gives a high concentration of stars at $7-9$ kpc distance. Note however, that this concentration is located at a mean distance slightly larger than 8 kpc. While 8 kpc (Wesselink 1987) has been adopted in the HRD-GST for the distance to the Galactic Centre (Ng et al. 1995). The displacement of the mean concentration of stars beyond 8 kpc is due to the fact that the differential volume increases with the distance.

Figures 2a – 2c show the different forms of extinction adopted for this analysis. In all these figures we show, as a reference, the 'actual' extinction (Ng et al. 1996a) as a thick line. Figure 2a shows the linear and step-like extinction. We consider three cases: the extinction is increased linearly or stepwise to the maximum value $A_V = 1\overset{m}{.}75$ at a distance 1, 2 or 4 kpc away from us.

The resolution of the input, patchy extinction map is scaled dynamically in a 200×200 grid between the minimum and maximum values. A smooth map is obtained through an appropriate interpolation scheme between the neighbouring points. The current choice of the figure dimensions results in an apparent, in distance, extended extinction patch. In the simulations 300 Poissonian distributed points are used as centers for these patches. Around these points another group of points are distributed within a radius λ. This radius actually defines how independent the patches are from each other. The patches give rise to the threaded like substructures in Fig. 2c, when they start to overlap with each other.

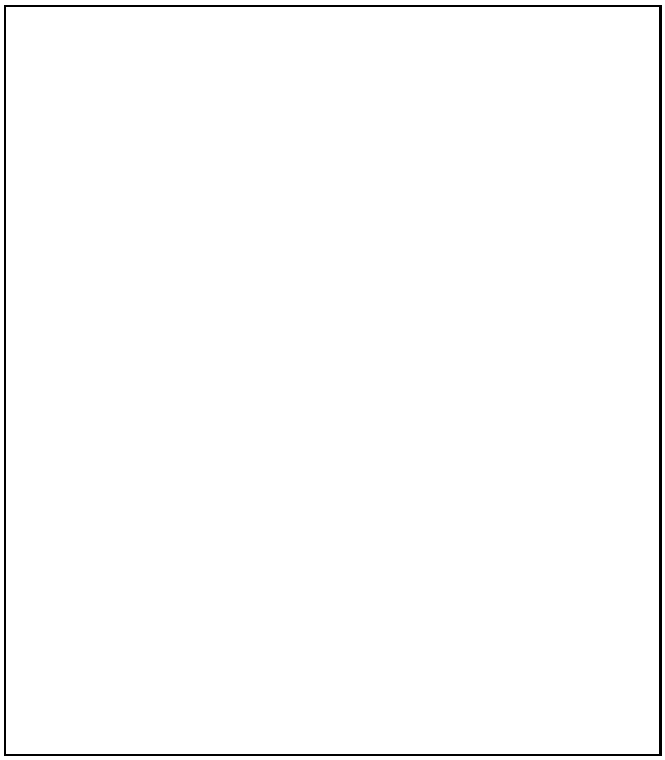

Fig. 3.3. Synthetic (V,V–I) CMD with a linearly increasing extinction up to $A_V = 1\overset{m}{.}75$ at 4 kpc distance

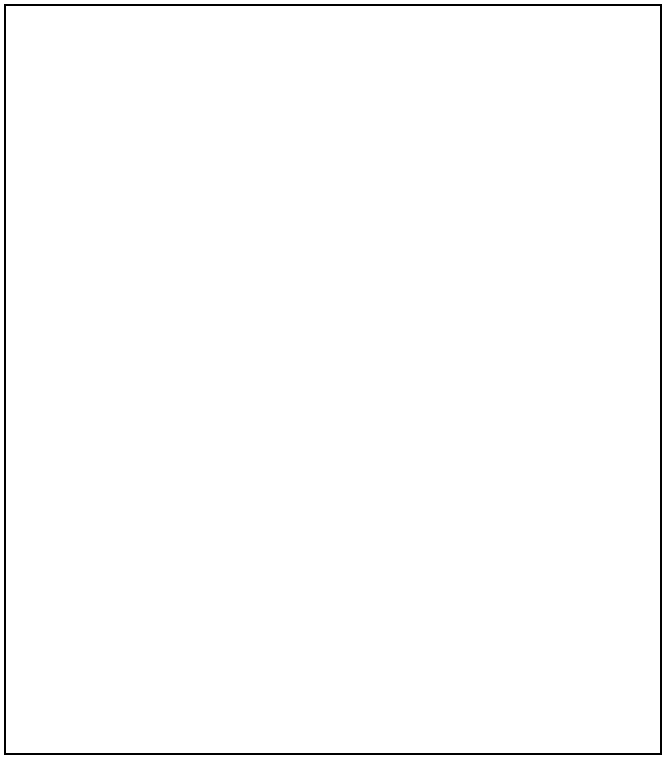

Fig. 4.1. Synthetic (V,V–I) CMD with a discretely increasing extinction up to $A_V = 1\overset{m}{.}75$ at 1 kpc distance

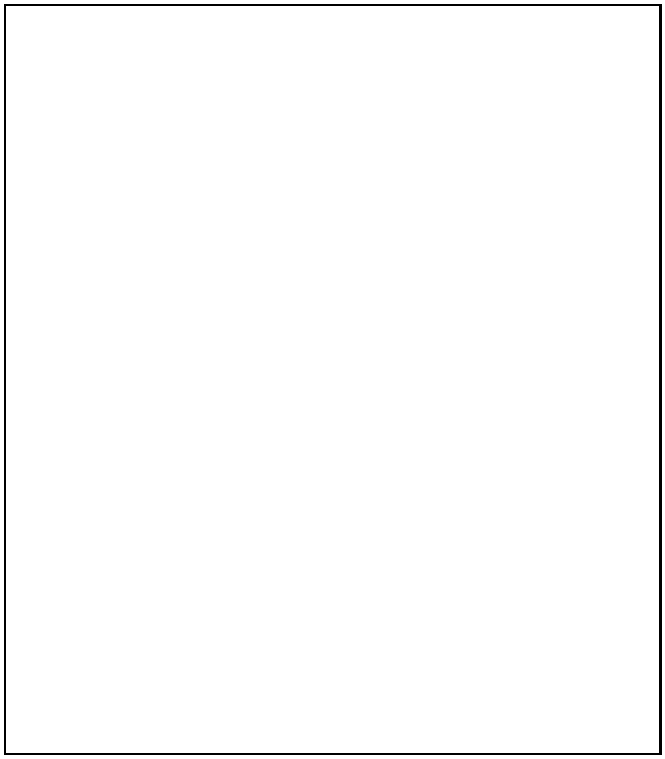

Fig. 4.2. Synthetic (V,V–I) CMD with a discretely increasing extinction up to $A_V = 1\overset{m}{.}75$ at 2 kpc distance

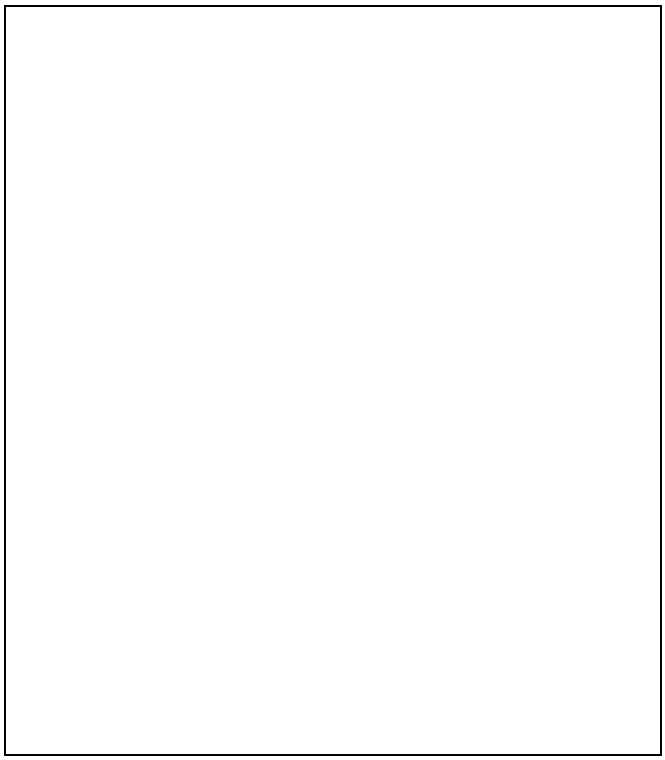

Fig. 4.3. Synthetic (V,V–I) CMD with a discretely increasing extinction up to $A_V = 1\overset{m}{.}75$ at 4 kpc distance

2.2. Results

Figures 3.1 – 3.3, 4.1 – 4.3, 5.1 & 5.2 and 6.1 & 6.2 show the resulting CMDs for the different type of extinction adopted.

Figures 3.1 – 3.3 show the CMD when a linear extinction curve is used. These figures show the cases where the extinction increases linearly, up to the maximum value at respectively 1, 2 and 4 kpc away from us. They further show the gradual tilt of the disc main sequence, up to the distance where the extinction is maximum. The sequence is vertical beyond that distance. Notice that the tilt of the disc main sequence has not the same orientation as the reddening vector. This is due to differences in both the extinction and the distance of each star. With an increasing distance for the maximum extinction, the disc horizontal branch stars along the line of sight start to disperse, because they do not have the same extinction. They also get a tilt, similar to the main sequence stars. Figs. 1.1 and 3.3 are quite similar, this is due to the fact that in first order the linear increasing extinction gives a good approximation to the actual extinction (see Fig. 2a).

With a 4 kpc distance for maximum extinction and $b = -4\overset{\circ}{.}2$ (Baade's Window, subfield #3) the outer boundary of this absorption layer is about 300 pc. This is in agreement with an effective thickness of 100 pc for an exponentially decreasing density distribution. It is emphasized that there is a discontinuity between the disc and the bar horizontal branches, because we did not include the simulations of the older disc populations. But this is merely an artifact caused by the simplifications

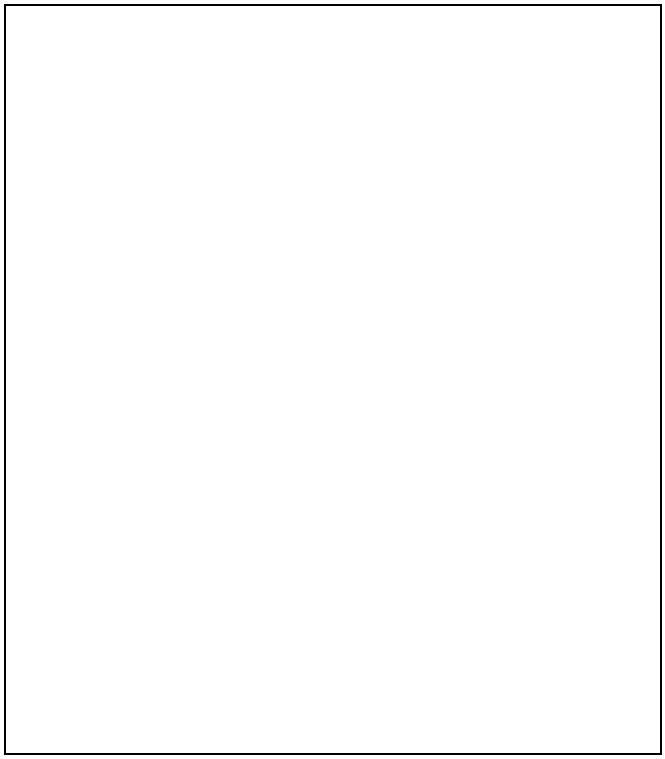

Fig. 5.1. Synthetic (V,V–I) CMD with a Poissonian distributed extinction ($A_V = 0\overset{m}{.}0 - 1\overset{m}{.}75$)

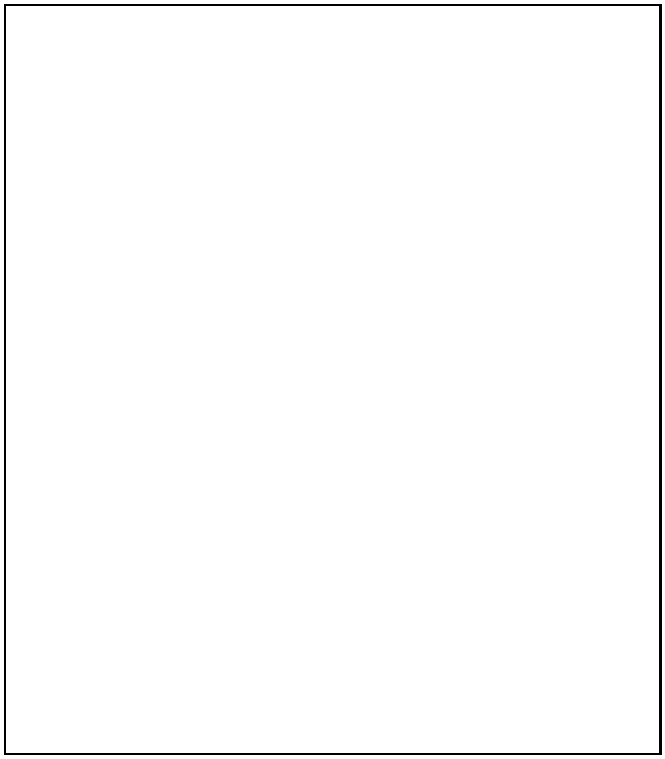

Fig. 5.2. Synthetic (V,V–I) CMD with a Poissonian distributed extinction ($A_V = 1\overset{m}{.}60 \pm 0\overset{m}{.}20$)

made for these simulations. The morphological structures of the bar population remain the same, because all the stars are located outside the extinction layer and all have a maximum extinction.

Figures 4.1 – 4.3 show the CMD when a step-like extinction curve is used. They show the cases for which the extinction increases suddenly, up to the maximum value at respectively 1, 2 and 4 kpc away from us. Due to the discrete step size of the extinction, the disc sequence splits up in two separate vertical sequences: one bluer (V–I $\simeq 0\overset{m}{.}6$) and brighter than the other (V–I $\simeq 1\overset{m}{.}25$), because the brighter stars are located in front of the extinction screen. Note that the two sequences are shifted from each other along the reddening line. The bright, blue sequence still connects with the fainter redder one through the lower mass main sequence stars (the dots in the figures). In contrast to the previous cases with a linearly increasing extinction, there is now a clear separation between the evolved stars from the disc and bar population. In Fig. 4.3 one can clearly see the disc turn-off from the stars which are located in front of the extinction screen. Also in these cases the morphological structures from the bar population remain the same, because all the stars are located behind the extinction layer and all have a maximum extinction.

In general, one does not have merely a step-like increase of the extinction. A combination with a gradual, with distance increasing extinction is more realistic. Due to the very distinct nature of the step-like increase in the extinction, one can determine quite accurately with an uncertainty of about 0.2 kpc the distance to the source of this feature. Bertelli et al. (1995) demonstrated this for the extinction of the field near the galactic cluster NGC 6603. The morphology of the disc sequence in the CMD of the cluster Terzan 1 (Ortolani et al. 1993) suggests that this is possibly another field, in which we can expect a step-like increase for the extinction at a certain distance. However, the analysis of the frame near this cluster (Bertelli et al. 1995) did not reveal the presence of a steep increase in the extinction along the line of sight. This probably is an other indication, that the extinction towards the galactic centre changes rapidly over a relatively small area.

Figures 5.1 & 5.2 show the CMDs for Poissonian extinction. In the first case A_V is varied between $0\overset{m}{.}0$ and $1\overset{m}{.}75$. It is emphasized once more that this exercise is not representative for the actual situation in Baade's Window. The adopted boundary of the absorbing layer is located at about 4 kpc away from us and, with respect to Fig. 3.3, the extinction can be lower at any given distance. The blue side of the disc structure will not be as tilted anymore and is nearly vertical now. Near the Galactic Centre some of the stars will be brighter and bluer, which can be clearly seen in the horizontal branch of the bar population. In Fig. 5.2 constraints are put to the lower limit of the extinction variations. This case is quite similar to Fig. 3.3, the only difference is that a dispersion is present around the mean extinction. This give rise to a little bit more dispersed morphology of the sequences in the synthetic CMD, but it will not introduce a change of the main morphological properties. The mean extinction for the bar stars in this simulation is lower

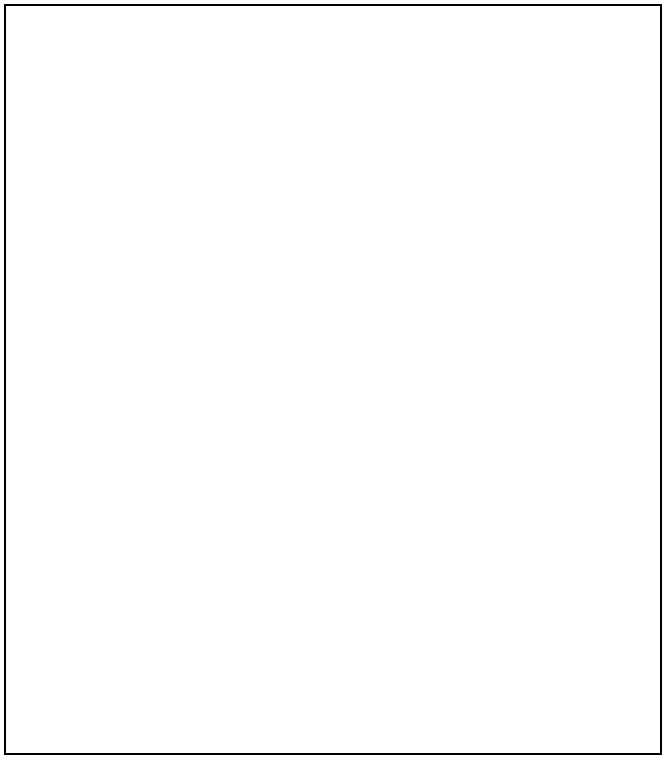

Fig. 6.1. Synthetic (V,V–I) CMD with a patchy extinction ($\lambda = 0.3$; $A_V = 1\overset{m}{.}60 \pm 0\overset{m}{.}20$)

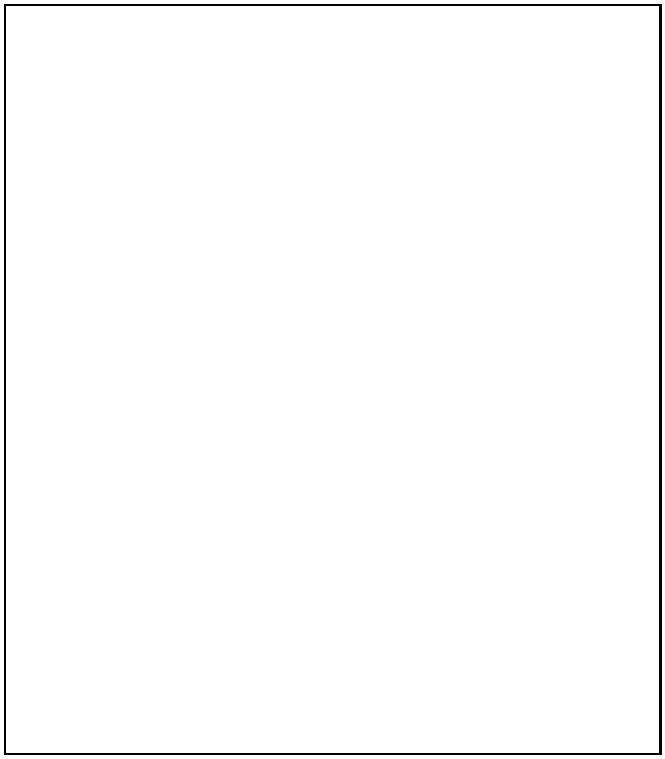

Fig. 6.2. Synthetic (V,V–I) CMD with a patchy extinction ($\lambda = 0.3$; $A_V = 1\overset{m}{.}80 \pm 0\overset{m}{.}50$)

than for Fig. 3.3. This results in a small blueward shift ($0\overset{m}{.}06$) of the bar population in Fig. 5.2 with respect to Fig. 3.3.

In the simulations of patchy extinction, A_V has been varied between $0\overset{m}{.}0$ and $1\overset{m}{.}75$ together with the correlation radius, respectively $\lambda = 0.3$ and 0.6, between the patches. The figures with $\lambda = 0.3$ and 0.6 are very similar. They differ in small details concerning substructures in the morphology of the different sequences in the CMD. Besides very small substructures, the CMDs are very similar to the Poissonian case in Fig. 5.1 and they are therefore not displayed. This result is not surprising, because all that matters is the extinction range. The extinction patches only give rise to some small substructures in the synthetic CMD. Similar arguments can be given for simulations with $A_V = 1\overset{m}{.}60 \pm 0\overset{m}{.}20$ and $\lambda = 0.3$ or 0.6 with respect to Fig. 5.2. The differences between patchy and random extinction are even smaller than in the previous case. Figure 6.1 shows the case $\lambda = 0.3$. For Fig. 6.2 an extinction range A_V between $1\overset{m}{.}3$ and $2\overset{m}{.}3$ is adopted. Again no big differences between the figures with $\lambda = 0.3$ or 0.6 are noticeable. We therefore consider only the case $\lambda = 0.3$. Because of the extinction range, this figure ought to be compared with the CMD from Baade's Window for the whole field, see for example Fig 1.1 (Ng et al. 1996a). Taking into account a $0\overset{m}{.}07$ shift in (V–I) colour (Ng et al. 1996a), partly due to differences in the zeropoint of the HRD-GST photometric system, between the simulated and the observed CMD, the following is noticed: the simulated RGB and HB both cover the corresponding region in the observed CMD completely.

This implies that $A_V = 1\overset{m}{.}3 - 2\overset{m}{.}3$ covers indeed the extinction in Baade's Window. It also confirms that the stars from the 'bar' population are dominating the RGB and HB morphological structures in the CMD. This does not imply that even metal-richer stars are absent in this field. It mainly shows that they are not dominantly present in the CMD. This is in agreement with the metallicity distribution found from Baade's Window K-giants (Sadler et al. 1996). Furthermore, the sequence due to the disc HB stars becomes broader and actually constrains the maximum extinction allowed along the line of sight.

The simulations in Figs. 6.1 & 6.2 show that the actual choice of the correlation radius, besides the very small values, is likely not very important. On the other hand, if only a small number of patches had been used, the results might have shown some dependency with the choice of the value for the correlation radius λ. But probably this is not a realistic option. Figures 6.1 & 6.2 further demonstrates that the HB morphology is due to differential reddening, combined with a metallicity spread among the HB stars. We are able to generate in the simulations a patchy like pattern for the extinction along the line of sight. If the extinction difference between the patchy 'globules' is large enough and when these globules are big enough, one of the questions that remains open for future analysis is: can we actually determine the distance to these patchy globules? In Baade's Window there is no big difference between a patchy or a Poissonian type of extinction. Only, when a large extinction range is present the difference might become noticeable.

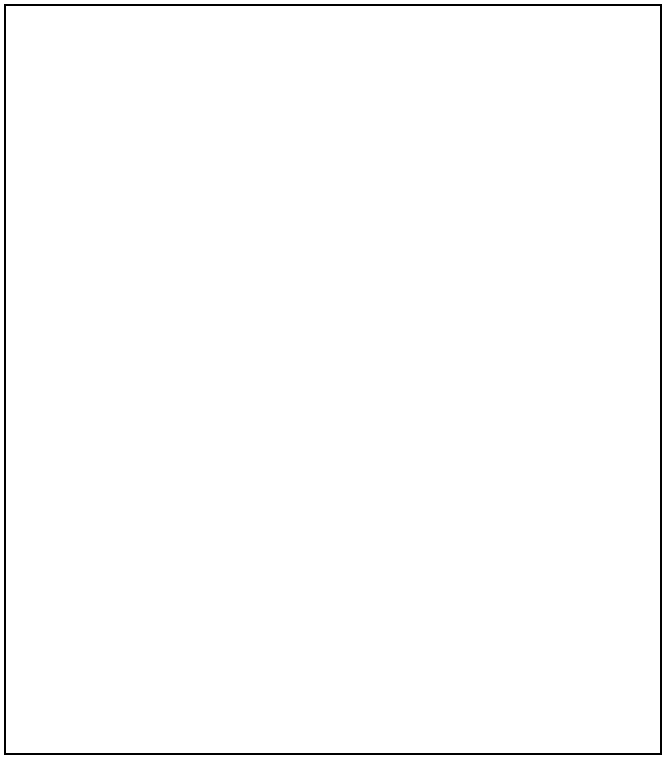

Fig. 7. Synthetic (J,J–K) CMD for Baade's Window. The absorption in the J and K passbands are obtained under the assumption that A_J/A_V = 0.282 and A_K/A_V = 0.112 (Rieke & Lebofsky 1985), with $A_V = 1\overset{m}{.}70$.

3. Discussion

MC simulations have been made for various types of extinction. The main extinction is caused by material inside an absorbing layer. In first order the boundary of this layer is at $z \simeq 300$ pc. The stellar contribution in this layer is due to disc stars from various populations along the line of sight. Any significant change in the extinction will show up clearly in the CMD morphology of the foreground disc sequence. But towards the galactic centre and Baade's Window this will only hold up to approximately a 5 kpc distance from the Sun, where a significant decrease in the disc density appears to be present (Bertelli et al. 1995; Ng et al. 1996a). For practical purposes one might assume a constant extinction beyond 5 kpc. On the other hand, the bari-centre of the bulge/bar red HB sequence provides information of the extinction at 8 kpc distance. A suitable interpolation, between this and the extinction at about 5 kpc, results in the extinction curves obtained in star counts studies with the HRD-GST.

If the red horizontal branch stars in Baade's Window is due to stars with a mean solar metallicity one has to disperse the horizontal branch stars along the reddening line and introduce a dispersion in the extinction, i.e. differential reddening. In that case, a smaller dispersion will be also present in the foreground extinction. If the dispersion is too large the disc sequence will change significantly. On the other hand, a small extinction dispersion, which is comparable with the colour dispersion of the disc sequence, will not give rise to a significant change in both the disc and bar morphology.

Patchiness of the extinction might be such, that it may introduce a change in the CMD the horizontal branch morphology of a population which has a mean solar metallicity, without influencing significantly the disc sequence. But this will require very special conditions for the patchiness of the extinction. One can imagine that these requirements can be found in a certain direction, but they will not be ubiquitous. An inspection of the CMDs from the various subfields in and near Baade's Window (Udalski et al. 1993), some offset fields near globular clusters (Ortolani et al. 1990, Bica et al. 1994) and the CMDs of metal-rich globular clusters (Ortolani et al. 1990, 1992, 1993, 1994, 1995b & 1996) shows that differences in the (mean) extinction are certainly present.

The horizontal branches from the field and the clusters all seem share something in common. It is unlikely that the change in the extinction is always such that the disc sequence in the CMDs is not influenced significantly, while the horizontal branches are dispersed along the direction of the reddening line. In fact the morphology of the disc sequence is always affected first by any change in the reddening. It is more likely that we are dealing with an underlying population which has, due to primarily a metallicity spread, a horizontal branch almost parallel to the extinction line. This population, such as the 'bar' population identified by Ng et al. (1996a&c), will not require special patchy extinction conditions. Ng et al. (1996d) demonstrated for metal-rich globular clusters that a stellar population similar to the 'bar' population can give a proper description of the cluster HBs. But one ought to be cautious with clusters at distances near 8 kpc. In those cases the cluster HB-clump overlaps with the bulge/bar clump and it will be difficult to separate the two contributions from each other (Ng et al. 1996d).

If one insists on a small metallicity range, a larger extinction range, $\Delta A_V \simeq 0\overset{m}{.}7$, will be required along the line of sight, in order to obtain a comparable morphological appearance for the cluster HBs. Such an increase in the extinction range will certainly affect the morphology of the disc sequence. The current analysis allows a change in the extinction of $\Delta A_V \simeq 0\overset{m}{.}2 - 0\overset{m}{.}3$. Such a value invokes only marginal changes in the morphology of the disc sequence in Figs. 6.1 and 6.2. Merely differential reddening or a large metallicity range will not be sufficient to explain the red HB morphology. This constraint therefore favours a large metallicity range combined with differential reddening.

In (V,V–I) CMDs age-metallicity and extinction effects cannot be separated unambiguously from each other when a large metallicity spread is present. Observations in other near infrared passbands are needed. In a (J,J–K) CMD extinction effects and metallicity effects are not pointing in the same direction. A simulated (J,J–K) CMD in Fig. 7 indicates that a horizontal spread in colour of the red horizontal branch stars is likely due to metallicity effects, while the effects of extinction will give a dispersion in another direction. Further-

more, the morphology of the (K,J–K) CMD of NGC 6528 from Guarnieri et al. (1995) indicates that this cluster probably has an almost constant extinction. The colour dispersion of the horizontal branch stars is likely due to age-metallicity effects. On the other hand, the large near infrared sky surveys (DENIS, Epchtein et al. 1993; 2MASS, Kleinmann 1992) might be suitable to study the variations of the extinction in large areas. Thus providing stronger constraints for the determination of the ages and metallicities of the stellar populations towards the Galactic Centre. The simulated (J,J–K) CMD, displayed in Fig. 7, shows that a study like this is feasible, even with $K_{lim} = 14\overset{m}{.}5$.

Simulations have been presented for different types of extinction. These simulations show that distinct differences are present between the morphology of the disc sequences for the different forms of extinction. They further show that the disc sequence is a good indicator for the nearby extinction along the line of sight. The difference between patchy and Poissonian extinction is not significant enough, in order to explain the HB-clump morphology in Baade's Window solely by patchy, differential extinction. Differential extinction combined with a metallicity spread among the HB stars is favoured as explanation for the red HB morphology.

Acknowledgements. Y.K. Ng is indebted to R. van de Weygaert for providing an algorithm to generate correlated distributions. Once more I made good use of it by generating patchy extinction maps. K.Z. Stanek is acknowledged for his constructive comments. Y.K. Ng thanks the Padova Astronomical Department for its hospitality. ANTARES, an astrophysics network funded by the HCM programme of the European community, provided financial support for Ng's research visit to Padova. Ng is supported by HCM grant CHRX-CT94-0627 from the European Community. G. Bertelli acknowledges the financial support received from the Italian Ministry of University, Scientific Research and Technology (MURST).

References

Arp H., 1965, ApJ 141, 43
Bertelli G., Bressan A., Chiosi C., Fagotto F., Nasi E., 1994a, A&AS 106, 275
Bertelli G., Bressan A., Chiosi C., Ng Y.K., Ortolani S., 1994b, Mem.S.A.It. 65, 689
Bertelli G., Bressan A., Chiosi C., Ng Y.K., Ortolani S., 1995, A&A 301, 381 (Paper II)
Bertelli G., Bressan A., Chiosi C., Ng Y.K., 1996, A&A 310, 115
Bica E., Ortolani S., Barbuy B., 1994, A&A 283, 67
Catalan M., de Freitas Pacheco J.A., 1996, PASP 108, 166
Cox D.P., Proceedings IAU Symposium 120, *'Structure and Dynamics of the Interstellar Medium'*, 17 – 21 April 1989, Granada (Spain), G Tenorio-Tagle, M. Moles and J. Melnick (eds.), 500
Epchtein N., et al., 1993, DENIS bluebook
Guarnieri M.D., Montegriffo P., Ortolani S., Moneti A., Barbuy B., Bica E., 1995, The Messenger 79, 26
Jones T.J., Ashley M., Hyland A.R., Ruelas-Mayorga A., 1981, MNRAS 197, 413
Kleinmann S.G., 1992, Proceedings *' Robotic telescopes in the 1990s'* 103rd Annual Meeting of the Astronomical Society of the Pacific, Univ. of Wyoming, Laramie, June 22-24, 1991, A.V. Filippenko (ed.), ASP Conference Series 34, 203
Ng Y.K., 1994, Ph.D. thesis, Leiden University, the Netherlands
Ng Y.K., 1996, Proceedings 'The impact of large-scale near-IR sky surveys', 24 – 26 April 1996, Puerto de la Cruz (Tenerife; Spain), P. Garzon-lopez (ed.), *in press*
Ng Y.K., Bertelli G., Bressan A., Chiosi C., Lub J., 1995, A&A 295, 655 (Paper I; erratum A&A 301, 318)
Ng Y.K., Bertelli G., Chiosi C., Bressan A., 1996a A&A 310, 771 (Paper III)
Ng Y.K., Bertelli G., Chiosi C., Bressan A., 1996b, A&A *submitted*
Ng Y.K., Bertelli G., Chiosi C., Bressan A., 1996c, Workshop 'Spiral Galaxies in the near IR', Garching bei München, 7–9 June 1995, D. Minniti and H.-W. Rix (eds.), 110
Ng Y.K., Bertelli G., Chiosi C., 1996d, A&A *submitted*
Ortolani S., Barbuy B., Bica E., 1990, A&A 236, 362
Ortolani S., Bica E., Barbuy B., 1992, A&AS 92, 441
Ortolani S., Bica E., Barbuy B., 1993, A&A 267, 66
Ortolani S., Barbuy B., Bica E., 1994, A&AS 108, 653
Ortolani S., Renzini A., Gilmozzi R., et al., 1995a, Nature 377, 701
Ortolani S., Barbuy B., Bica E., 1995b, Messenger 82, 10
Ortolani S., Barbuy B., Bica E., 1996, A&A 308, 733
Paczyński B., Stanek K.Z., Udalski A., et al., 1994, AJ 107, 2060
Renzini A., 1996, workshop 'Spiral Galaxies in the near IR', Garching bei München, 7–9 June 1995, D. Minniti and H.-W. Rix (eds.), 95
Rieke G.H., Lebofsky M.J., 1985, ApJ 288, 618
Sadler E.M., Rich R.M., Terndrup D.M., 1996, AJ *in press*
Stanek K.Z., 1996, ApJ 460, L37
Ruelas-Mayorga R.A., Rev. Mex. Astron. Astrofis. 22, 27
Udalski A., Szymański M., Kałużny J., Kubiak M., Mateo M., 1993, Acta Astron. 43, 69
Wesselink Th.J.H., 1987, Ph.D. thesis, Catholic University of Nijmegen, the Netherlands
Woźniak P.R., Stanek K.Z., 1996, ApJ 464, 233

This article was processed by the author(s) using Springer-Verlag TEX A&A macro package 1991.